

The last two terms in (3a) are again modified Fubini-Nambu-Wataghin terms included to guarantee gauge invariance. Utilizing the relations needed for deriving (4), we now obtain

$$M_{pv}^E = M_{ps}^E + ie\sqrt{2} g_{pv}(F_N - F_c)\bar{U}(p_f)\gamma_5[\not{\epsilon} - (k\cdot\epsilon)\not{k}/k^2]U(p_i), \quad (4a)$$

i.e.,  $M_{pv}^E \neq M_{ps}^E$  if  $F_N \neq F_c$ .

Equation (1a) with some further  $s$ -channel resonance contributions was used<sup>4</sup> to analyze recent electron production data.<sup>5</sup> With  $F_N$  taken from electron-proton scattering experiments it was possible to find  $F_\pi(k^2)$  giving a best fit. With Eq. (3a) possessing *two* unknown functions  $F_\pi(k^2)$  and  $F_c(k^2)$ , one may obviously improve the fit. One can then analyze whether  $F_c = F_N$  yields the best fit or rather  $F_c \neq F_N$ .

The last possibility would *definitely* indicate a pseudovector coupling whereas the first one does *not* exclude it.

<sup>1</sup>B. Richter, in *Proceedings of the Third International Symposium on Electron and Photon Interactions at High Energies, Stanford Linear Accelerator Center, Stanford, California, 1967* (Clearing House of Federal Scientific and Technical Information, Washington, D. C., 1968), p. 313.

<sup>2</sup>J. J. Sakurai, in *Proceedings of the Fifth Annual Eastern Theoretical Physics Conference*, edited by D. Feldman (Benjamin, New York, 1967), p. 81.

<sup>3</sup>S. Fubini, Y. Nambu, and V. Wataghin, *Phys. Rev.* **111**, 329 (1958); F. A. Berends and G. B. West, *Phys. Rev.* **188**, 2538 (1969).

<sup>4</sup>H. Fraas and D. Schildknecht, *Phys. Lett.* **35B**, 72 (1971); F. A. Berends and R. Gastmans, *Phys. Rev. Lett.* **27**, 124 (1971); R. C. E. Devenish and D. H. Lyth, *Phys. Rev. D* **5**, 47 (1972).

<sup>5</sup>C. Driver *et al.*, *Phys. Lett.* **35B**, 77, 81 (1971), and *Nucl. Phys.* **B30**, 245 (1971), and **B33**, 45, 84 (1971); P. S. Kummer *et al.*, *Lett. Nuovo Cimento* **1**, 1026 (1971); C. N. Brown *et al.*, *Phys. Rev. Lett.* **26**, 987 (1971).

## Tests of High-Energy Models by Two-Particle Analyses\*

Rudolph C. Hwa

*Institute of Theoretical Science and Department of Physics, University of Oregon, Eugene, Oregon 97403*

(Received 16 December 1971)

Two-particle distribution functions are calculated in the diffractive-excitation model and compared with those of the multiperipheral model. Optimum regions for differentiating the predictions of the models are indicated. Decisive, yet feasible, experimental tests are suggested.

Among the various models of multiparticle production at high energy,<sup>1</sup> two apparently conflicting ones are the multiperipheral model<sup>2</sup> (MPM) and the diffractive-excitation model<sup>3,4</sup> (DEM). Yet, despite their great differences many of their predictions are remarkably similar, e.g., the logarithmic dependence of average pion multiplicity on energy, and the limiting pion spectra. It is reasonable to expect that the differences between the models are likely to show up in the two-particle correlations among the final particles. Investigations in the two-particle distribution functions have been made<sup>5</sup> with particular emphasis on MPM or Mueller's generalization<sup>6</sup> of it. In this paper we calculate explicitly the two-particle distribution functions in DEM, indicate the restricted regions where the two models differ most

strongly, and suggest what crucial experimental quantities to measure.

In terms of the scaled c.m. longitudinal-momentum variable  $x = 2k_{\parallel}/\sqrt{s}$  for a single- or two-particle inclusive reaction, we define the (noninvariant) distribution functions to be

$$\rho_1(x) = d\sigma/dx, \quad \rho_2(x_1, x_2) = d\sigma/dx_1 dx_2. \quad (1)$$

Throughout this paper we shall be interested only in the pion distributions. We have

$$\int_{-1}^1 \rho_1(x) dx = \sum_n n \sigma_n \equiv \langle n \rangle \sigma_T, \quad (2)$$

$$\int_{-1}^1 \int_{-1}^1 \rho_2(x_1, x_2) dx_1 dx_2 = \sum_n n(n-1) \sigma_n \equiv \langle n(n-1) \rangle \sigma_T, \quad (3)$$

$$\int_{-1}^1 \rho_2(x_1, x_2) dx_2 \equiv \langle n(x_1) \rangle \rho_1(x_1), \quad (4)$$

where  $\langle n(x_1) \rangle$  is the average multiplicity per collision accompanying the detection of a particle at  $x_1$ .

Without specifying  $\rho_1$  or  $\rho_2$ , we already know  $\sigma_n$  for the MPM and DEM. In the MPM,<sup>2</sup>  $\sigma_n \propto (\ln s)^n/n!$  so that  $\langle n \rangle \propto \ln s$  and  $\langle n(n-1) \rangle \propto (\ln s)^2$ . On the other hand, in the DEM,<sup>3</sup>  $\sigma_n \propto n^{-2}$  for large  $n$ , so that  $\langle n \rangle \propto \ln s$  also, but  $\langle n(n-1) \rangle \propto \sqrt{s}$ . The difference in the predictions of  $\langle n(n-1) \rangle$  can be experimentally checked, but probably cannot be firmly distinguished in the near future.

In the MPM it is usually assumed that the two-particle correlation is short ranged.<sup>5</sup> Denoting rapidity<sup>7</sup> by  $r$ , i.e.,

$$r = \ln(k^0 + k_{\parallel})/M, \tag{5}$$

where  $M$  is the proton mass, the correlation length  $l$  in  $r$  is estimated to be  $l=2$ . For  $\Delta r > l$  there is no correlation, and one has (assuming a factorizable Pomeranchukon)

$$\rho_2(x_1, x_2) = \sigma_T^{-1} \rho_1(x_1) \rho_1(x_2). \tag{6}$$

For  $\Delta r < l$  the correlation is important and (6) is invalid. What  $\rho_2$  should be in that region is not specified in general, since the prescription of it is not among the endowed attributes of the MPM.

For a description of  $\rho_2$  in the DEM we first note that<sup>4</sup>

$$\rho_1(x) = \int (d\sigma/dn_1 dn_2) [g(n_1; x)n_1 + g(n_2; x)n_2] dn_1 dn_2, \tag{7}$$

where  $g(n_i; x)$  is the probability density (whose integral over  $x$  is unity) of finding a pion at  $x$  in the  $i$ th cluster of  $n_i$  pions,  $i=1, 2$ . Extending the counting to the two-particle case, we have

$$\rho_2(x_1, x_2) = \int (d\sigma/dn_1 dn_2) \{ [g(n_1; x_1)g(n_2; x_2) + g(n_1; x_2)g(n_2; x_1)] n_1 n_2 + g(n_1; x_1, x_2)n_1(n_1-1) + g(n_2; x_1, x_2)n_2(n_2-1) \} dn_1 dn_2, \tag{8}$$

where  $g(n_i; x_1, x_2)$  is the probability density of finding one pion at  $x_1$  and another at  $x_2$  among the  $n_i$  pions in the  $i$ th cluster; its normalization is  $\int_{-1}^1 g(n_i; x_1, x_2) dx_2 = g(n_i; x_1)$ . Equations (7) and (8) are actually quite general and have validity beyond the confines of the DEM. It is straightforward to show that they satisfy (2) and (3).

Under the assumption that the Pomeranchukon is factorizable we have  $d\sigma/dn_1 dn_2 = \sigma_T^{-1} (d\sigma/dn_1) \times (d\sigma/dn_2)$ .<sup>8</sup> In DEM the probability density  $g(n_i; x)$  is assumed to be a Gaussian distribution in the rest frame of the  $i$ th cluster. In the spirit of the statistical interpretation associated with the pion-emission processes of the excited states, we further assume that, when  $n_i$  is large,

$$g(n_i; x_1, x_2) = g(n_i; x_1)g(n_i; x_2), \tag{9}$$

i.e., the particles are emitted independently. Since  $d\sigma/dn_i$  and  $g(n_i; x)$  are known functions,<sup>4</sup>

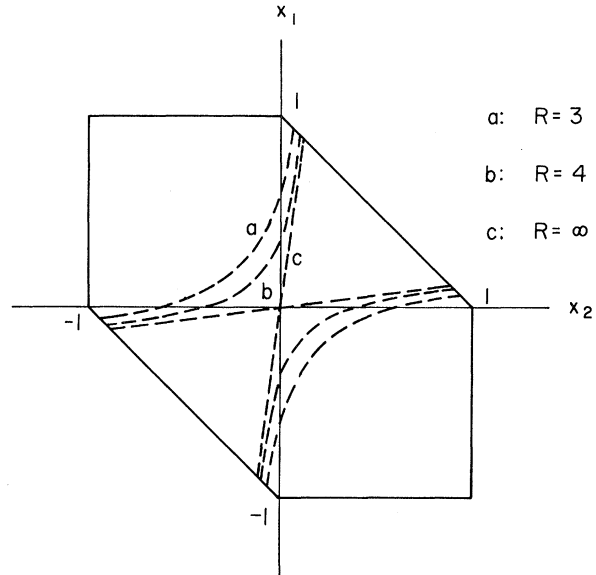


FIG. 1. Longitudinal phase space of two-pion inclusive reactions in  $pp$  collisions. The "benzene-ring" kinematical boundary is for asymptotic energy. Dashed lines correspond to  $|\Delta r|=2$  for various values of total rapidity  $R$ .

which lead to striking predictions on  $\langle n \rangle$ ,  $\rho_1$ (pion), and  $\rho_1$ (proton) without free parameters,  $\rho_2$  is therefore completely specified.

It is widely recognized that the rapidity variable  $r$  has many virtues. However, because the range of  $r$  increases as  $\ln s$ , it is inconvenient to present scaling behavior in an  $r$  plot. In the scaled variables  $x_1$  and  $x_2$ , not only are the maximum variations in  $\rho_1$  and  $\rho_2$  fully exhibited, the regions where two-particle correlations are important can also be clearly seen in an  $x_1$ - $x_2$  plot. In Fig. 1 we show the kinematically allowable region of such a plot, the boundaries of which at asymptotic energy are  $x_1 + x_2 = \pm 1$  in the "parallel" regions, and  $|x_1| = |x_2| = 1$  in the "antiparallel" regions. Dashed lines indicate  $|\Delta r| = |r_2 - r_1| = l = 2$  for various energies or total rapidity  $R = \ln(s/M^2)$ , where  $M$  is the proton mass for  $pp$  colli-

sions.

In the MPM the short-range two-particle correlation is important only in the region between the hyperbolic curves. In the limit  $s$  or  $R \rightarrow \infty$ , that region is restricted to the triangular areas bounded by  $\ln(x_2/x_1) = l = 2$ . Indeed, the fact that the ratio  $\mu = x_2/x_1$  is just  $\exp(r_2 - r_1)$  for  $k_{\parallel} \gg k_{\perp}$  makes  $\mu$  a very useful variable, which will be exploited in the following.

At infinite energy  $\rho_2$  is very clear-cut in the

$$\rho_2(x_1, x_2) = \int (d\sigma/dn_1) g(n_1; x_1, x_2) n_1(n_1 - 1) dn_1. \quad (10)$$

We shall show in the next section that the correlation is strong in the DEM throughout the *entire* parallel regions.

For comparison with the MPM at asymptotic energy we are forced to the narrow sector  $0 < \mu < e^{-1} = 0.134$  (and its mirror images across symmetry axes), where (6) applies in the MPM. There is no general prediction by the MPM in the bulk of the parallel region of high correlation. Fortunately, the two models differ significantly in the narrow sectors to be amenable to experimental tests at high-enough energies such as those available at the National Accelerator Laboratory and intersecting storage rings. At nonasymptotic energies the distinctions between the two models become less pronounced, and the kinematical region worthy of special attention fades out. This circumstance cannot be avoided by a different choice of variables.

Let us make the calculation in the DEM for the  $pp$  collision at asymptotic energy. In evaluating (10) we use<sup>3,4</sup>  $d\sigma/dn_1 = An_1^{-2}$  for large  $n_1$ , where  $A$  is a constant, and

$$g(n_1; x) = (\alpha/\pi)^{1/2} n_1 \exp[-\alpha(n_1 x - 1)^2], \quad (11)$$

where  $\alpha \equiv \langle k_{\parallel} \rangle^2 / \langle k_{\perp}^2 \rangle \approx \frac{3}{2}$ . By virtue of (9) we obtain for  $x_1$  and  $x_2 > 0$

$$\rho_2(x_1, x_2) = (A\alpha/\pi) e^{-\alpha(2-c)} \int_{n_0}^N dn_1 n_1(n_1 - 1) \exp[-\alpha c(\nu n_1/c - 1)^2], \quad (12)$$

where

$$c \equiv (1 + \mu)^2 / (1 + \mu^2), \quad \mu \equiv x_2/x_1, \quad \nu \equiv x_1 + x_2. \quad (13)$$

$N$  is the maximum multiplicity proportional to  $\sqrt{s}$ . We stress that  $\mu$  is defined only in the parallel regions where it is positive. In evaluating the integral in (12), we keep  $\nu$  away from the wee- $x$  region, i.e.,  $|\nu| > N^{-1}$ . We obtain the limiting distribution

$$\rho_2(x_1, x_2) = \frac{Ac^2}{2\pi\nu^3} \exp[-\alpha(2-c)] \left\{ \frac{1}{2} \left( \frac{\pi}{\alpha c} \right)^{1/2} [1 + 2\alpha(c-\nu)] \operatorname{erfc} \left[ \sqrt{\alpha c} \left( \frac{\nu}{c} n_0 - 1 \right) \right] + \left[ \frac{\nu}{c} (n_0 - 1) + 1 \right] \exp \left[ -\alpha c \left( \frac{\nu}{c} n_0 - 1 \right)^2 \right] \right\}, \quad (14)$$

where  $\operatorname{erfc} X = 1 - \operatorname{erf} X$ , and  $n_0$  is the multiplicity of the minimal cluster.

What is significant in (14) is the  $\nu^{-3}$  behavior at small  $\nu$  independent of  $\mu$  in the parallel region. This is to be contrasted from the form if there is no correlation. Approximating  $\rho_1(x_i)$  by  $x_i^{-1}$  at small  $x_i$ , one has

$$\sigma_T^{-1} \rho_1(x_1) \rho_1(x_2) \propto (x_1 x_2)^{-1} = (1 + \mu)^2 / \mu \nu^2 \quad (15)$$

which has only a  $\nu^{-2}$  behavior. Thus the DEM is a model with strong correlations: (6) is invalid in the parallel region for any value of  $\mu$ , i.e., any rapidity difference. We note that (14) is limiting, therefore scaling in  $s$ . However, it has no simple scaling property in  $x_1$  relative to  $x_2$ . Whereas the invariant distribution  $x_1 x_2 \rho_1(x_1) \rho_2(x_2)$  does not depend on  $\nu$ , the true two-particle invariant distribution  $x_1 x_2 \times \rho_2(x_1, x_2)$  in the DEM does depend on  $\nu$ . Hence, it is inappropriate to describe the strength of two-particle correlation in terms of only the rapidity difference  $\Delta r$  or the variable  $\mu$ .

In the MPM  $\rho_2(x_1, x_2)$  is given by (6) and (15) in the region  $0 \leq \mu \leq 0.134$ . It is a weakly correlated

DEM. All particles with  $x > 0$  belong to the forward-going cluster, and all with  $x < 0$  to the backward-going cluster; there is no overlap. In the antiparallel regions in Fig. 1, (6) then prevails, exactly as prescribed by the MPM. Experiments for distinguishing the two models should therefore concentrate on probing the parallel regions. In the forward region, for example,  $\rho_2$  is given exclusively by the third term in (8), i.e., for  $x_1$  and  $x_2 > 0$ ,

model.

It is also of interest to focus upon the  $\mu$  dependences in the two models. For clarity we integrate out  $\nu$ , thereby also increasing the statistics of data when a comparison with experiments is to be made in the future. We define

$$\rho(\mu, \nu) d\mu d\nu = \rho_2(x_1, x_2) dx_1 dx_2, \quad (16)$$

$$h(\mu) = \int_{\nu_0}^1 \rho(\mu, \nu) d\nu, \quad (17)$$

where  $\nu_0 \sim O(s^{-1/2})$ . We obtain from (14), or more directly from (12),

$$h(\mu) = \frac{A}{2\pi\nu_0} e^{-2\alpha} \left( \frac{1+\mu}{1+\mu^2} \right)^2 \left[ 1 + \frac{1}{2} \left( \frac{\pi}{\alpha c} \right) (1+2\alpha c) e^{\alpha c} (1 + \operatorname{erf} \sqrt{\alpha c}) \right]. \quad (18)$$

Evidently  $h(\mu) \propto \sqrt{s}$ , just as we have anticipated for  $\langle n(n-1) \rangle$  since the integral of  $h(\mu)$  over  $\mu$  converges. Indeed, (18) indicates that in the DEM  $h(\mu)$  decreases, as  $\mu \rightarrow 0$ , and approaches a constant apart from the  $\sqrt{s}$  factor. On the other hand, the MPM predicts from (6) and (15) that in the region  $0 \leq \mu \leq 0.134$ , one has

$$h(\mu) \propto \mu^{-1} \ln \nu_0 \propto \mu^{-1} \ln s \quad (\text{MPM}). \quad (19)$$

It diverges as  $\mu \rightarrow 0$ . Indeed, this is how  $\langle n(n-1) \rangle \propto \ln^2 s$  obtains in the MPM when (19) is integrated over  $\mu$ .

The  $\mu$ ,  $\nu$ , and  $s$  dependences discussed here should all be checked experimentally, especially at intersecting-storage-ring energies where the predictions of the two models are more reliable.

In certain experiments it is easier to measure the exclusive multiplicity  $\langle n(x) \rangle$  defined in (4). Theoretically, although it is possible to obtain this quantity by working from (14), numerically if necessary, it is physically more appealing to proceed as follows. From (11) we see that the peak of the  $x$  distribution for a given cluster of  $n_1$  pions is located at  $\langle x \rangle \sim 1/n_1$ . This means that if a pion is observed at  $x$ , most likely  $1/x$  number of pions has been produced in association with the observed one during the same collision, not counting the pions produced in the other cluster. Since on the average each cluster is responsible for half the total average multiplicity  $\langle n \rangle$ , which increases as  $\ln s$ , we obtain

$$\langle n(x) \rangle = a/|x| + \frac{1}{2} \langle n \rangle. \quad (20)$$

Note that since  $\rho_1(x) \sim 1/x$  at small  $x$ , integration of (4) over  $x_1$  yields the consistent result  $\langle n^2 \rangle \propto \sqrt{s}$  in the DEM. On the other hand, in order that  $\langle n^2 \rangle$  may behave as  $(\ln s)^2$  as in the MPM, the  $1/x$  behavior in (20) is precluded. Equation (20) should be tested immediately; at present energies the  $|x|^{-1}$  factor should be rounded off near  $x=0$ .

Assuming that a proton detected at small  $x_p$  is roughly at rest in a cluster, we also obtain a for-

mula similar to (20) for the exclusive pion multiplicity associated with the detection of a proton at small  $x_p$ .

We have identified a number of quantities of interest in two-particle analyses:  $\langle n^2 \rangle$ ,  $\rho_2$  at small  $x_1+x_2$ ,  $h(\mu)$  at small  $x_2/x_1$ ,  $\langle n(x) \rangle$ , and  $\langle n(x_p) \rangle$ . The regions of importance are for very small or very large ratios of  $x_2/x_1$  in the parallel regions. Measurements of these quantities in these regions are feasible and decisive in testing of the two models. We await the judgment of our experimental colleagues.

\*Work supported in part by the U. S. Atomic Energy Commission under Contract No. AT(45-1)-2230.

<sup>1</sup>For a review see, for example, W. Frazer *et al.*, to be published.

<sup>2</sup>D. Amati, A. Stanghellini, and S. Fubini, *Nuovo Cimento* **26**, 896 (1962); C. E. DeTar, *Phys. Rev. D* **3**, 128 (1971).

<sup>3</sup>R. C. Hwa, *Phys. Rev. Lett.* **26**, 1143 (1971).

<sup>4</sup>R. C. Hwa and C. S. Lam, *Phys. Rev. Lett.* **27**, 1098 (1971).

<sup>5</sup>H. Abarbanel, *Phys. Rev. D* **3**, 2227 (1971); A. Mueller, *Phys. Rev. D* **4**, 150 (1971); D. Z. Freedman *et al.*, *Phys. Rev. Lett.* **26**, 1197 (1971); A. Basseto, M. Toller, and L. Sertorio, *Nucl. Phys. B* **34**, 1 (1971).

<sup>6</sup>A. Mueller, *Phys. Rev. D* **2**, 2963 (1970).

<sup>7</sup>This definition of rapidity follows essentially that of J. D. Bjorken [*Particles and Fields—1971*, AIP Conference Proceedings No. 2, edited by A. C. Melissinas and P. F. Slattery (American Institute of Physics, New York, 1971), and SLAC Report No. SLAC-PUB-974, 1971 (unpublished)]. It differs from the usual  $y$  variable (DeTar, Ref. 2) by an additive factor  $\ln(k_1^2 + m^2)^{1/2}/M$ .

<sup>8</sup>This form follows from Eq. (8) in Ref. 4, which differs from Eq. (9) of Ref. 3 essentially in only one respect. That is, we have neglected the dependence of  $\beta(t)$  on  $M_1$  and  $M_2$ . Such a dependence, as expressed by Eq. (8) of Ref. 3, was a rough guess for small  $M_1$  and  $M_2$ . We now believe that  $B$  should become a positive constant for  $M_{1,2} \gtrsim 2$  GeV so that the factorizability of  $d\sigma/dn_1 dn_2$  follows at large  $n$ .